



# Parametric Investigation of Closed Loop Pulsating Heat Pipe with Cerium Oxide Nanofluid

M. Madhuri<sup>†</sup> and N. P. Yadav

*Bundelkhand Institute of Engineering & Technology, Jhansi, U.P., 284128, India*

<sup>†</sup>Corresponding Author Email: [madhuri.me17@gmail.com](mailto:madhuri.me17@gmail.com)

(Received April 2, 2022; accepted June 11, 2022)

## ABSTRACT

In this study, a closed-loop pulsating heat pipe experimental investigation was done with 1% wt concentration of cerium oxide/EG-water (60-40) nanofluid. The unsteady state measurement was done to determine the effect of heat input, filling ratio and evacuation pressure on the thermal performance of the closed-loop pulsating heat pipe. The thermal performance is assessed in terms of temperature variation, thermal resistance and effective thermal conductivity of the pulsating heat pipe. The most appropriate behaviour is observed at 0.0799 bar evacuation pressure with 50% FR. The lowermost thermal resistance of 0.116598K/W was observed at 0.0799 bar evacuation pressure and 50% FR. The effective thermal conductivity value was observed as 5078.34 W/mK at 50% FR, 0.0799 bar for 80W heat input which is 12 to 13 times better than pure copper. The pulsation action inside the pulsating heat pipe is verified with the power spectral density analysis. This study supports the better performance of the heat pipe at 50% FR with a lower evacuation pressure of 0.0799 bar.

**Keywords:** Thermal management; Pulsating heat pipe; Nanofluid; Cerium Oxide; FFT.

## NOMENCLATURE

A	area	$T_c$	condenser wall temperature
$D_o$	pipe diameter	$T_e$	evaporator wall temperature
$l$	pipe length	$c$	condenser
T	temperature	CLPHP	Closed Loop Pulsating Heat Pipe
$Q_{in}$	heat input	$e$	evaporator
$th$	thermal resistance	FR	Filling Ratio
$L_{eff}$	effective length	PHP	Pulsating Heat Pipe
$K_{eff}$	effective thermal conductivity		

## 1. INTRODUCTION

With the advancement in the electronics and semiconductor industry, and encroachment in the manufacturing of these components, the requirement of the compact size of the products can be met, but the increase in heat flux is a challenge to thermal management of the cooling system. Therefore, to meet the cooling demand of the industries, research works are going on various novel concepts of cooling technologies. The heat pipe is a very efficient compact device that can transfer a high amount of heat from a higher temperature source to a lower temperature source or environment without consuming the outsource energy (Li *et al.* 2020).

The heat pipe technology is developed early in the 1960s. There have been many changes in its shape

and structure. In the 1990s, Akachi developed a passive heat transfer device known as pulsating heat pipe (Akachi 1990). The pulsating heat pipe is referred to as a superconductor owing to its high effective thermal conductivity and it helps to remove the excess heat from the heat source (Nazari *et al.* 2018; Ahmad *et al.* 2010). The pulsating heat pipe is constructed with a long capillary tube bent to form several turns and filled with the fluids for different ratios. PHP is classified as an open-loop and a closed-loop; if both the pipe ends are joined together, it is a closed-loop; otherwise, it is an open loop. Several scholars believe that CLPHP is better than others because of the proper circulation of fluid within the pipe (Bastakoti *et al.* 2018a). The heat gain on the evaporator is shifted towards the condenser section, wherever it cools. The existence of a temperature gradient causes pressure variation

within the tube, which is responsible for the growth, generation and collapse of the bubble (slug and plug generation). PHP does not merely dissipate the fluid's latent heat though it also dissipates the liquid's sensible heat. So, the flow of working fluid in pulsating heat pipe originated due to the oscillation and phase change phenomenon of the working fluid. The PHP has various applications in microelectronics cooling, solar system and automotive technology (Qu *et al.* 2021; Agha 2011).

The researchers performed various experimental and theoretical analyses to know the PHP thermal performance. PHP thermal performance is affected by various parameters, which are, i.e., heat input, working fluid, Filling Ratio, diameter, orientation, no of turns, tube material, length of the evaporator, adiabatic and condenser, evacuation pressure, as suggested by Bao *et al.* (2020), Bastakoti *et al.* (2018b), Naik *et al.* (2013), Sun *et al.* (2017) and Narasimha *et al.* (2012), Kwon and Kim (2015). The working fluid with high conductivity, i.e., nanofluid, helps in improving the pulsating heat pipe thermal performance. The nanofluid is the fluid in which metallic and non-metallic nanoparticle size ranging less than 100 nm is added to the base fluid with the one-step or two-step method (Taha-Tijerina 2018). Nanofluids have wide applications for efficient cooling in electronic components, space and advanced cooling systems conferred to Ciloglu (2017). The results showed that CeO<sub>2</sub>, Al<sub>2</sub>O<sub>3</sub>, and their hybrid nanofluids had higher thermal conductivity enhancement percentages (3.3%, 5.3%, and 8.8%) at volume conc. of 0.5% and temperature (50°C) for deionized water (Kamel *et al.* 2021). Numerous nanofluids can be employed in PHP.

The presence of nanoparticles in the base fluid increases the nucleation locations and gets stronger the nucleation boiling; because of this overall thermal performance of the heat pipe is increased (Riehl and Santos 2012). Ciloglu (2017) has done an experimental study to know the pool boiling features of cerium oxide nanoparticles. The heat transfer coefficient in pool boiling increases in the presence of Ce<sub>2</sub>O nanofluid. The critical heat flux increases up to 103% for 0.1 volume% concentration of cerium oxide nanofluid compared to deionised water. The critical heat flux is the location where the overheating arises because the vapour bubbles completely enclose the heating surface. The nano-particles conc. also plays a vital role in thermal performance. Some researchers says that low conc. of nanoparticles improves the thermal performance i.e., Jia *et al.* (2013) look into the influence of SiO<sub>2</sub>/H<sub>2</sub>O nanofluid in PHP. They found that with high conc. of SiO<sub>2</sub>/H<sub>2</sub>O deteriorate the PHP performance and vice versa. Whereas some researchers found that a high concentration of nanoparticles improves thermal performance. Harun *et al.* (2019) and Li *et al.* (2020) reported that the heat transfer coefficient and thermal performance of PHP increase as the nanoparticle concentration increases in the nanofluid. Nine *et al.* (2014) investigated the effect of different conc. (0.5-3%)

wt. with cu/water nanofluid in the PHP. From the analysis, it was found that with 2% wt. concentration nanofluids shows optimum performance. Ramesh *et al.* (2017) have studied nanofluid (0.01% CeO<sub>2</sub>/water volumetric fraction) for the flat plate water heater. A substantial enhancement is observed in the performance with forced circulation compared to the traditional method at a low volumetric fraction. The thermal performance increased by 9.3% with the addition of 0.01% volumetric fraction cerium oxide nanofluid; similar results were reported by Gupta *et al.* (2019) and they found that the cerium oxide nanofluids reduce the wall temperature and thermal resistance of heat pipe when dispersed with water. Shojaei *et al.* (2019) used 60 ppm cerium oxide nanofluid and 5% water with B5 (95% diesel fuel and 5% Biodiesel) fuels to reduce CO, HC and NO<sub>x</sub> emissions. Cerium oxide nanofluid also applies as an additive in the B5 fuels.

Krishna *et al.* (2017) have discussed the use of Al<sub>2</sub>O<sub>3</sub> up to 1% with Tricosane in the heat pipe. Tricosane with a 1% concentration of Al<sub>2</sub>O<sub>3</sub> as PCM can recover the 53% power utilisation of the fan. They observed that suitable suspension of nanoparticles in phase-changing material has a greater perspective for enhancement in the conventional energy storage systems. So, the nanoparticles help increases the heat transfer capacity of the system. Ma *et al.* (2006 a, b) have studied 1.0% volume nano-diamond nanofluid in PHP. They observed the nanoparticle suspension was due to the fluctuation of the working fluid. The thermal resistance with nanofluids declines to 0.03 °C/W, and the thermal conductivity coefficient increases from 0.5813W/mK to 1.0032W/mK. The shape and size of nanoparticles are also crucial for heat transfer capacity. The cylinder shape nanoparticle contributes to extreme heat transfer performance. The performance efficiency improvement was 75.8%, and the minimum thermal resistance value was 0.113°C/W at 200W power input was found at 0.3% volume fraction of nanofluid (Ji *et al.* 2011a, b). Zufar *et al.* (2020) have evaluated the thermal behaviour of pulsating heat pipe with Al<sub>2</sub>O<sub>3</sub>-CuO (0.1%wt.) and SiO<sub>2</sub>-CuO (0.1%wt.) hybrid nanofluid and also compared it with water. SiO<sub>2</sub>-CuO nanofluid demonstrated the lowermost thermal resistance related to Al<sub>2</sub>O<sub>3</sub>-CuO nanofluid and water. SiO<sub>2</sub>-CuO nanofluid shows lowermost thermal resistance, which was 57% lesser than water and 34% lesser than Al<sub>2</sub>O<sub>3</sub>-CuO nanofluid at 80W heat input and 60% FR. The lowest thermal resistance was 0.27 °C/W for SiO<sub>2</sub>-CuO nanofluid. The optimal FR for all the heat input and FR was 60%. Hybrid nanofluids show a faster start-up phenomenon and lower evaporator temperature difference with a lower thermal resistance (Zufar *et al.* 2019). Akbari and Saidi (2019) have reported that heat pipe material and working fluids temperature are crucial factors for stabilising the nanofluids. The more stable nanofluid shows better thermal performance and less stable nanofluid shows the worst thermal performance compare to the base fluid. They also show that there is no prominent effect of nanofluid on the flow pattern of

the fluid inside the pipe. The best thermal performance is observed for titania/water nanofluid at 70% FR with 70W heat input.

Li et al. (2020) did an experimental analysis of PHP with graphene-water ethylene glycol nanofluid with 0.1 g/l to 2 g/l for heat input range 10-100W. They observed that with the increases in the concentration the thermal resistance decreases and thermal heat coefficient increases. The response surface methodology model is employed to improve thermal performance by lowering thermal resistance. The nanofluids have many advantages in heat transfer fields, some disadvantages also exist such as, when high conc. of nanoparticles are added to the base fluid; viscosity of the nanofluid increases and nanoparticles can erode the working fluid passage (Akbari and Saidi 2019).

The majority of the earlier experimental work was primarily engrossed in the issues influencing the behaviour of PHP, i.e., number of turns, working fluids, conc. and size and shape of the nanoparticles, heating mode, filling ratio, heat load and its restriction in the form of evaporator dry-out and section length etc. the purpose of the current study is to know the cerium oxide nanofluid effect on the thermal performance with the varying filling ratio and evacuation pressure. To the author's knowledge, there has been no research on thermal performance with the potential of cerium oxide/water/ethylene glycol (by volume 40:60) as occupied fluid within a pulsating heat pipe with changing evacuation pressure.

This research aimed to learn more about cerium oxide nanofluid's thermal performance and potential in the PHP at various filling ratios and evacuation pressures with varying heat input. The purpose of the power spectral study was to better understand the pulsation behaviour inside the heat pipe and how it affects its thermal performance.

## 2. EXPERIMENTAL SETUP

A closed-loop pulsating heat pipe setup is designed for this experiment. The PHP is constructed with a copper tube and has 5 turns. The internal and external diameter for PHP is 5mm & 6.8mm, respectively and pipe thickness is 0.9mm. The inner diameter should satisfy the criteria specified by Liu et al. (2015). The copper pipe has a three-zone, i.e., evaporator, adiabatic and condenser with lengths of 90mm, 140mm & 60mm, respectively.

The entire setup consists of a PHP, heating element, DAQ system, temperature measurement system, evacuation, and the charging system displayed in Figure 1. The evaporator section is wound by Ni-Cr wire (500W) to supply power by variable AC power supply (Variac, SERVOKON type 0-270 & Max Load- 8AMPS) as a heat source. A DAQ system is used to record the temperature in the computer using Lab VIEW 15.1 software. The evaporator and adiabatic section are entirely shielded with glass wool, and the condensation section is fully open to losing the heat to the environment. K-type thermocouples (13 no.) are assembled at various

positions in the evaporator (5 no.), adiabatic (2 no.) and condenser section (5 no.) to measure the temperature of the heat pipe, as presented in Figure 1. The evaporator section thermocouple positions are from 1 to 5, condenser section thermocouple positions are from 8 to 12 and adiabatic section thermocouple positions are 6 and 7. The condenser section is covered with a duct and the surrounding temperature inside the duct is measured by 0 location. The vacuum pump evacuates the CLPHP for pressure from 0.0799 bar to 1.0132 bar. The experiments were completed to explore the thermal behaviour of CLPHP at different pressure (0.0799-1.0132 bar) and the filling ratio of 30%-90% for various power inputs (10 W-90 W) with Cerium oxide nanofluid as a working fluid.

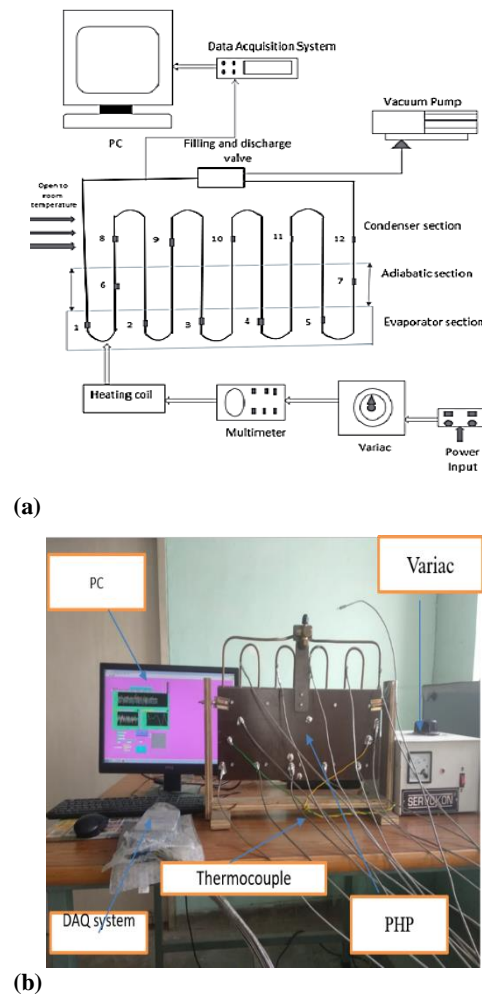


Fig. 1. (a) PHP schematic (b) Experimental setup of the pulsating heat pipe (Yadav et al., 2019).

### 2.1 Preparation of Nanofluid

Cerium oxide nanoparticles have many industrial applications, including heat exchangers, heat transfer, fuel cells and coolant material (Çiloğlu 2017). In the present study, cerium oxide/EG-water nanofluid was procured by a nano research lab. Table 1 lists the properties of cerium oxide nanoparticles. The cerium oxide nanoparticle

concentration was 1% by weight. The base fluid is a 40/60 volume mix of water and ethylene glycol. The ultrasonic oscillator is used to mix cerium oxide nanoparticles in the base fluid to create the nanofluid. A magnetic stirrer is used to agitate the nanofluid for 3-4 hours prior to each experiment to prevent the nanofluid from aggregating on the pipe wall. As a result, no sedimentation was observed for 4-5 days after the magnetic stirring. The magnetic stirrer homogenizes the nanofluid and then filled into the pulsating heat pipe for the current experiment.

**Table 1 Property of cerium oxide nanoparticles**

Parameters	Value
Colour	Light yellow
Particle size	30nm-50nm
True Density	6.5gm/cm <sup>3</sup>
Bulk Density	1.3gm/cm <sup>3</sup>
Purity	99.9%
Specific surf area	40-50m <sup>2</sup> /g

**2.2 Procedure**

The PHP is evacuated with a vacuum pump, the pressure is maintained at the required pressure (0.0799-1.0132 Bar) and the working fluid is charged. The working fluid volume refers to a 30%-90% filling ratio (FR). Once the correct filling ratio volume and evacuation pressure are archived, the pipe is sealed. The variable power input (10W to 90W) is supplied to the evaporator section through the heater at different voltages with the help of variac. The experiments are directed with cerium oxide nanofluid till the system reaches a steady-state. The temperature is recorded at various locations through a DAQ system up to which a steady state is attained.

**3. RESULTS AND DISCUSSION**

The experiments have been done with different conditions, and the CLPHP behaviour is evaluated in the form of thermal resistance (R<sub>th</sub>). A system can confine heat flow from the system and calc as given in 'Equation (1)'.

$$R_{th} = \frac{T_e - T_c}{Q} \tag{1}$$

T<sub>e</sub> is the evaporator, and T<sub>c</sub> is the condenser's average steady-state temperatures as calculated by 'Equations (2) & (3)'.

$$T_e = \frac{1}{5} \sum_5^1 T_i \tag{2}$$

$$T_c = \frac{1}{5} \sum_{12}^8 T_i \tag{3}$$

Where i is of thermocouples locations on evaporator (e), condenser (c) and Q is the power supply in the evaporator section by the heating coil. The heat input is an essential parameter in generating the pulsation inside the PHP. The continuous pulse is caused due to the pressure gradient inside PHP. However, even though the system has reached a steady-state, the temperature fluctuations were still observed in the evaporator and condenser section. The CLPHP has 5 thermocouples on the evaporator, 2 on the adiabatic section and 5 on the condenser. The CLPHP is mounted with 5 thermocouples on the evaporator and 5 on the condenser section and 2 on the adiabatic section. Therefore, uncertainty in evaporator temperature and condenser temperature is calculated by given 'Equation (4) & (5)' (Kline et al. 1953).

$$\%U_e = \sqrt{\left(\frac{\Delta T_1}{T_1}\right)^2 + \left(\frac{\Delta T_2}{T_2}\right)^2 + \left(\frac{\Delta T_3}{T_3}\right)^2 + \left(\frac{\Delta T_4}{T_4}\right)^2 + \left(\frac{\Delta T_5}{T_5}\right)^2} \tag{4}$$

$$\%U_c = \sqrt{\left(\frac{\Delta T_8}{T_8}\right)^2 + \left(\frac{\Delta T_9}{T_9}\right)^2 + \left(\frac{\Delta T_{10}}{T_{10}}\right)^2 + \left(\frac{\Delta T_{11}}{T_{11}}\right)^2 + \left(\frac{\Delta T_{12}}{T_{12}}\right)^2} \tag{5}$$

The evaporator and condenser temperature uncertainty are calculated by 'Equation (4)' and 'Equation (5)', which is approximately 5%.

The vertical bottom mode heating was done with evacuation pressures (0.0799 - 1.0132 Bar) and 30% - 90% FR. The effect of many parameters i.e., filling ratio, heat input and evacuation pressure with cerium oxide nanofluid as a working fluid is discussed next section.

**3.1 Effect of Heat Input**

The evaporator and condenser wall temperature fluctuation concerning time is given in Fig.2 at 0.0799 bar and 30%FR. The heat input ranges from 10W-90W in Fig. 2. The temperature rises with an increase in heat input up to 1000sec. After that, we can see a pseudo-static condition that appears after 1000sec together for evaporator and condenser regions shown in Fig. 2. This periodic fluctuation with time represents the continuous pulsation within the heat pipe.

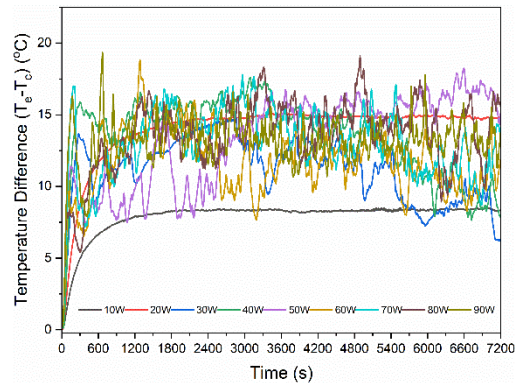


**Fig. 2. Evaporator and condenser temperature variation with time for different heat input at 0.0799 bar and 30% FR.**

It is found that there is higher temperature fluctuation at high heat input because of the frequent fluid flow. However, at low power input (10-20W) less heat flows from the wall to the fluid. So, fluctuation is significantly less since the occupied fluid flow is sluggish at low power input because of lesser energy; fluid takes extra time to travel from evaporator to condenser and appears as a straight line.

### 3.2 Evacuation Pressure Effect on Temperature

Evacuation pressure plays an essential role in the thermal performance of the PHP. The saturation temperature of the fluid decreases at low pressure and an early boiling phenomenon starts in the system. So, in the present analysis, the evacuation pressure is 0.0799 bar, 0.35 bar, 0.6132 bar and 1.0132 bar.

Figure 3 shows the evaporator and condenser temperature variation with time for 90W heat input and 30% FR at various evacuation pressure. At low evacuation pressure of 0.0799 bar, the evaporator saturation temperature is low compared to other evacuation pressure; therefore, at low-temperature fluids start boiling and form bubbles that flow into the condenser section due to the temperature difference between the evaporator and condenser section. In the condenser section, these bubbles collapse and a pressure gradient exist which helps in the proper circulation of the fluid. Figure 3(b) shows that the condenser temperature increases with a decrease in evacuation pressures because more heat is transported from the evaporator to the condenser in the presence of phase change due to lower saturation temperature at low evacuation pressure. Therefore, the pulsation effect inside the pipe is enhanced at low pressure and is responsible for high heat transfer.

### 3.3 Effect of Filling Ratio

The fluid's volume fraction inside the pipe is defined as the filling ratio. The filling ratio is categorized into three groups, i.e., 0%, 20-90% and 100% FR. 0% FR shows a conduction mode of heat transfer with higher thermal resistance, and 100% FR shows fewer bubbles form, which makes it behave like a thermosyphon. 20-90% FR shows the true working range suggested by Khandekar (2004). This study was done for FR in the range of 30-90%.

Figure 4 shows the temperature fluctuation with time at 0.0799bar and 90W with different filling ratios. The higher temperature fluctuations are observed at 30% and 50% FR and comparatively low at 70% and 90%. At 90% FR, there is minimal fluctuation because fewer bubbles are forming within the pipe due to the maximum portion of the pipe being covered with the working fluid. Conversely, the highest fluctuation encourages the pulsating effect observed at 50% FR because of more bubble formation.

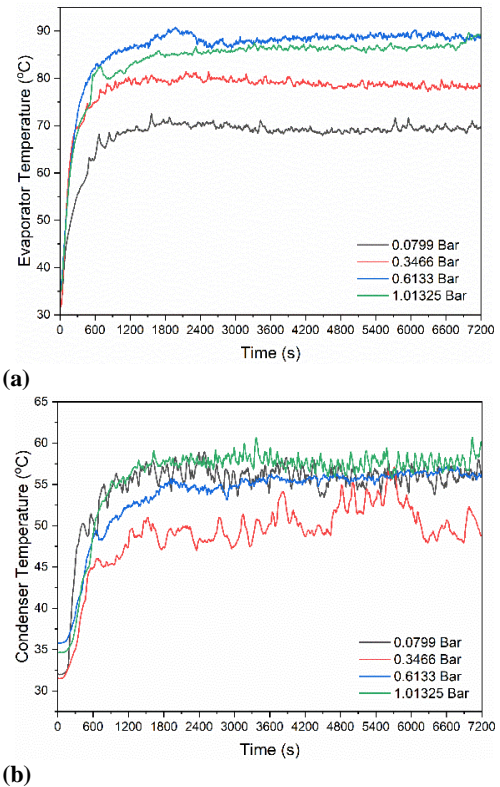


Fig. 3. Temperature variation for different evacuation pressure at 90 W heat input and 30% FR (a) Evaporator(b)Condenser.

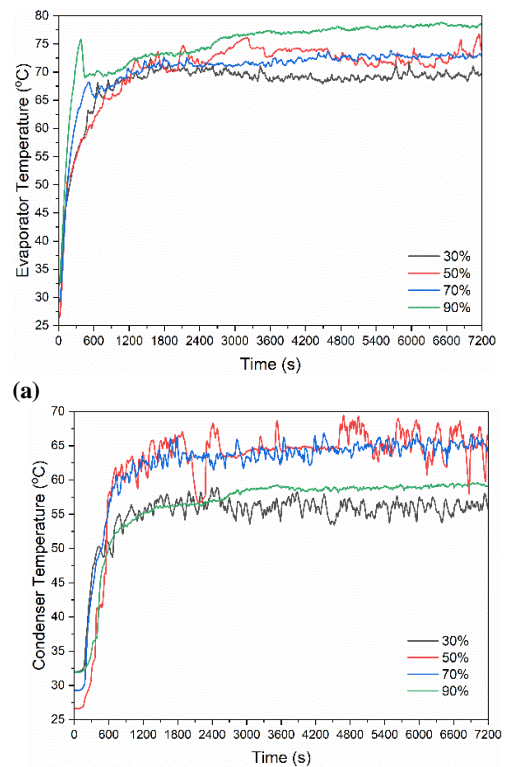


Fig. 4. Temperature variation with time at 0.0799 bar evacuation pressure and 90W heat input for different FR (a) Evaporator(b) condenser.

### 3.4 Evacuation Effect on Thermal Resistance

Thermal resistance is calculated by using equation 1. The thermal resistance variation with heat input at different FR with evacuation pressure is shown in Fig. 5 with standard deviation.

Figure 5 signifies the variation of the thermal resistance of PHP with increasing heat input. The thermal resistance declines nonlinearly with increasing heat input for the entire filling ratio (30% to 90%) given in Figs. 5(a) to 5(d). The reduction in the thermal resistance is due to the formation of vapour bubbles at the liquid-solid interface (Harun *et al.* 2019). The lowest thermal resistance is found at lower evacuation pressure 0.0799 bar which is 0.132243 K/W at 90W, 0.116598K/W at 80W, 0.131791K/W at 90W and 0.125142K/W at 60W for 30%, 50%,70% and 90% respectively. PHP shows asymptotic thermal resistance behaviour at lower vacuum pressure and the trend of thermal resistance is approximately similar for all the filling ratios at atmospheric pressure. The minimum thermal resistance is observed at 50% FR and 0.0799 bar for 80 W compared to other filling ratios. The minimum thermal resistance value for 0.0799 bar at 80W are 0.116598K/W, 0.159827K/W, 0.173731K/W and 0.224581K/W for 50%, 30%, 70% and 90% respectively. A small variation in thermal resistance is found at lower heat input (10W to 40W). Beyond 40W heat input, variation in thermal resistance is more due to intermittent motion of the fluid inside the PHP. Because the working fluid temperature is higher than the saturation temperature, causing a better pulsating effect inside the heat pipe.

### 3.5 Evacuation Pressure Effect on Effective Thermal Conductivity of PHP

The thermal behaviour of PHP is shown in terms of effective thermal conductivity. The heat input effect with various filling ratios and evacuation pressure on the effective thermal conductivity is displayed in Fig. 6 with standard deviation.  $K_{eff}$  for the PHP is calculated by Equation 9 (Jung *et al.* 2020 & Kwon and Kim 2015).

$$K_{eff} = \frac{Q_m \times L_{eff}}{A \times (T_{e,avg} - T_{c,avg})} \tag{6}$$

$$L_{eff} = L_a + \frac{L_e + L_c}{2} \tag{7}$$

$$A = 2n \frac{\pi}{4} D_o^2 \tag{8}$$

Effective thermal conductivity variation with heat input at unlike evacuation pressure with FR is displayed in Fig. 6. PHP effective thermal conductivity increases with increased heat input shown in Fig. 6. The effective thermal conductivity variation with heat input is nonlinearly at 0.0799 bar, whereas it is approximately linear for all the pressure (0.3466 bar, 0.6133 bar and 1.01325 bar). The highest effective thermal conductivity value is 5078.337W/mK at 50% FR with 0.0799 bar at 80W,

which means it is working 12 to 13 times better than pure copper (Mameli *et al.* 2014) for all the FR, the highest  $K_{eff}$  is at 0.0799 bar evacuation pressure. This is because there is a low-temperature difference between the evaporator and the condenser sections.

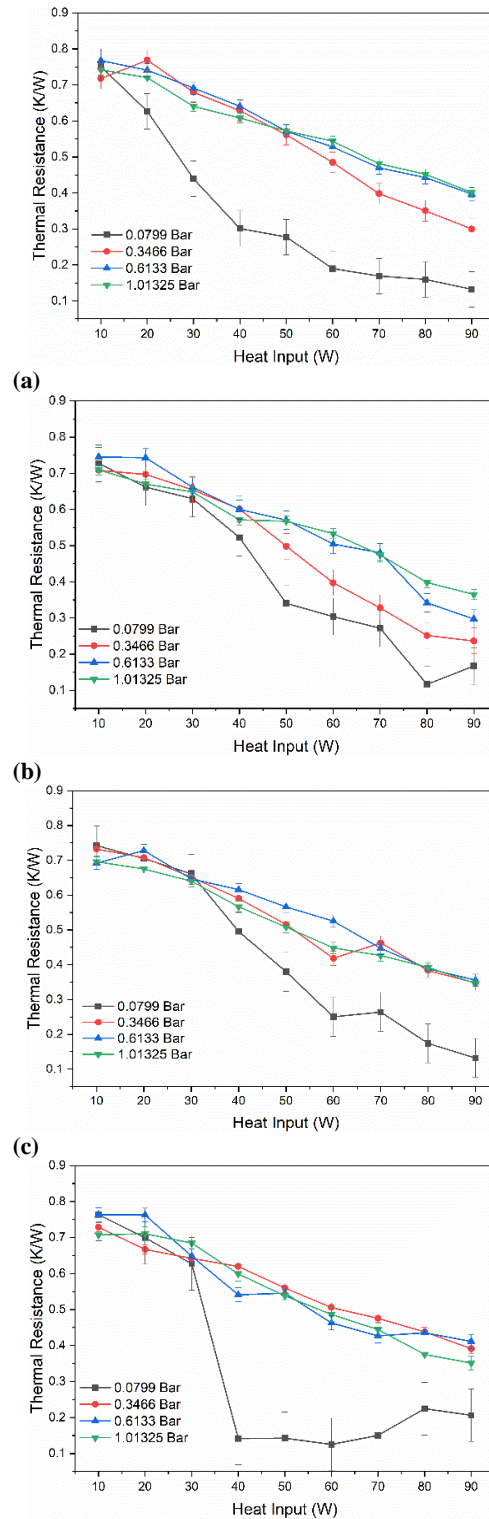
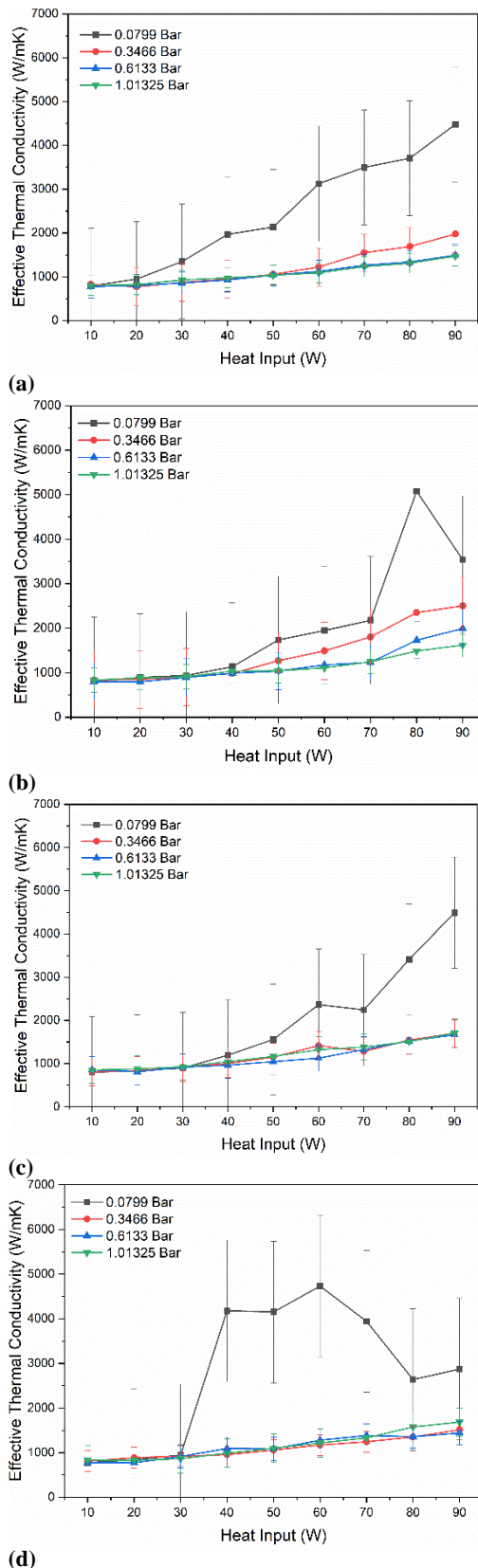


Fig. 5. Thermal resistance variation for different evacuation pressure (a) at 30% FR (b) at 50% FR (c) at 70% FR (d) at 90%FR.



**Fig. 6. Effective thermal conductivity variation for various evacuation pressure (a) at 30% FR (b) at 50% FR (c) at 70% FR (d) at 90%FR.**

### 3.6 Effect of Evacuation Pressure on Pulsation Frequency of PHP

The PSD investigation is conducted to identify the recurrent behaviour of a temperature fluctuation. The motion of the fluid is considered random when the power spectral is asymptotic and continuous. In contrast, it is periodic when it follows the Sharpe peak spreading at a leading frequency (Narasimha *et al.* 2012). The PSD investigation of temperature fluctuation in the steady-state region (beyond 1800 seconds) for the condenser section was done. The leading pulsation frequency and their magnitude are shown in Fig. 7 and Fig. 8 respectively, at a different evacuation pressure and FR from 30 to 90%. The leading frequency and magnitude are observed after the 40W heat input. At this heat input range, fluid reaches its saturation point for its evacuation pressure, as discussed in Fig 5. The dominant frequency is higher at higher heat input and increases with decrease in evacuation pressure. Figures 7 and 8 show the higher leading frequency and their magnitude at 50% FR followed by 70% and 30% because the temperature fluctuation at 50%, 70%, and 30% FR are higher, as displayed in Fig.4 (b). Due to this, higher thermal and conductivity minimum thermal resistance is found at 50%, with a 0.0799 bar given in Figs. 5 and 6.

The spectral power density variation with frequency is given in 9 (a) & 9 (b) for 80W heat input with 50% FR and 0.0799 bar and 1.01325 bar pressure. The frequency range was observed from 0-0.02 Hz. The leading frequency for Fig 9 (a) is 0.000541 Hz with a magnitude of 2.3, followed by the second-leading frequency observed at 0.001354 Hz with a magnitude of 1.13. The lower frequency value shows long vapour plug and liquid slug distribution in the PHP. Figure 9(b) shows the single leading frequency of very low magnitude (0.061) at the evacuation pressure of 1.01325 bar, which is about 18 times lesser than the second leading frequency magnitude at 0.0799 bar, reveals that the thermal performance of heat pipe at 0.0799 bar at 50% FR is better. This is also verified with temperature fluctuations with time at the same conditions as shown in Figure 10. The higher temperature fluctuations are observed at 0.0799 bar than 1.01325 bar.

### 4. CONCLUSION

The transient experimental measurement analysis of PHP was done to examine the pulsating heat pipe performance with cerium oxide/EG-water (60-40) nanofluid. The evacuation pressures, filling ratios, heat input and PSD analysis estimate the PHP's performance. The pulsation effect within the PHP was verified by temperature measurement at different locations with time at other operating conditions. The performance of the pulsating heat pipe is estimated by calculating the thermal resistance, effective thermal conductivity and dominant pulsation frequency and their magnitude.

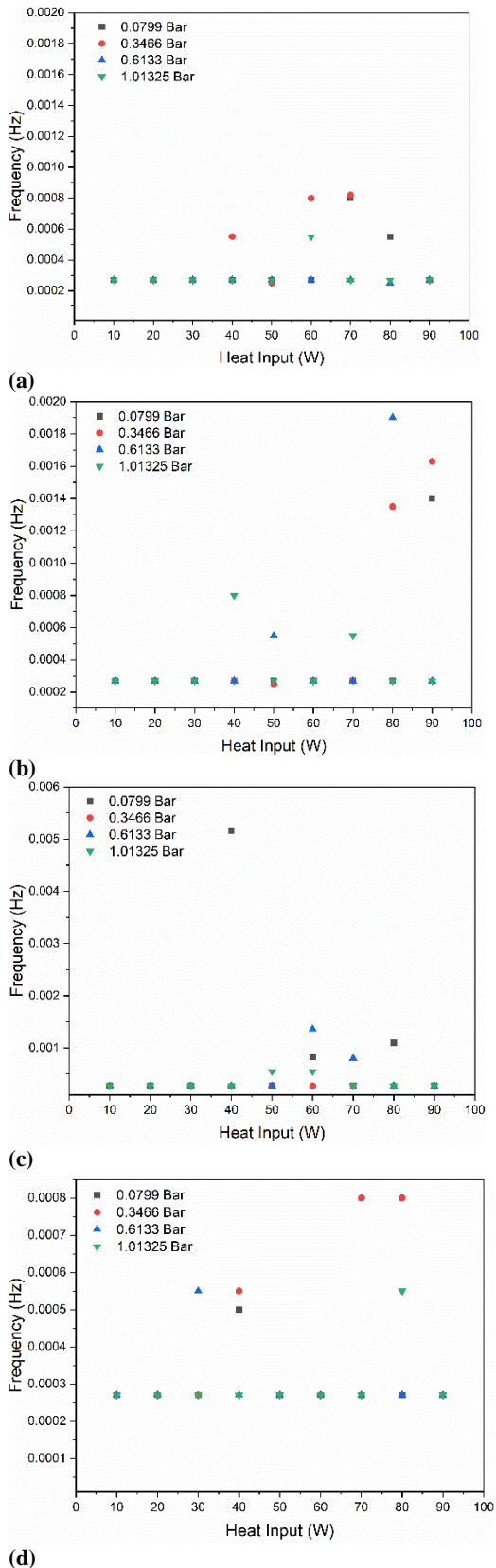


**Fig. 7. Dominant pulsation frequency variation for different evacuation pressure inside the condenser (a) at 30% FR (b) at 50% FR (c) at 70% FR (d) at 90%FR.**

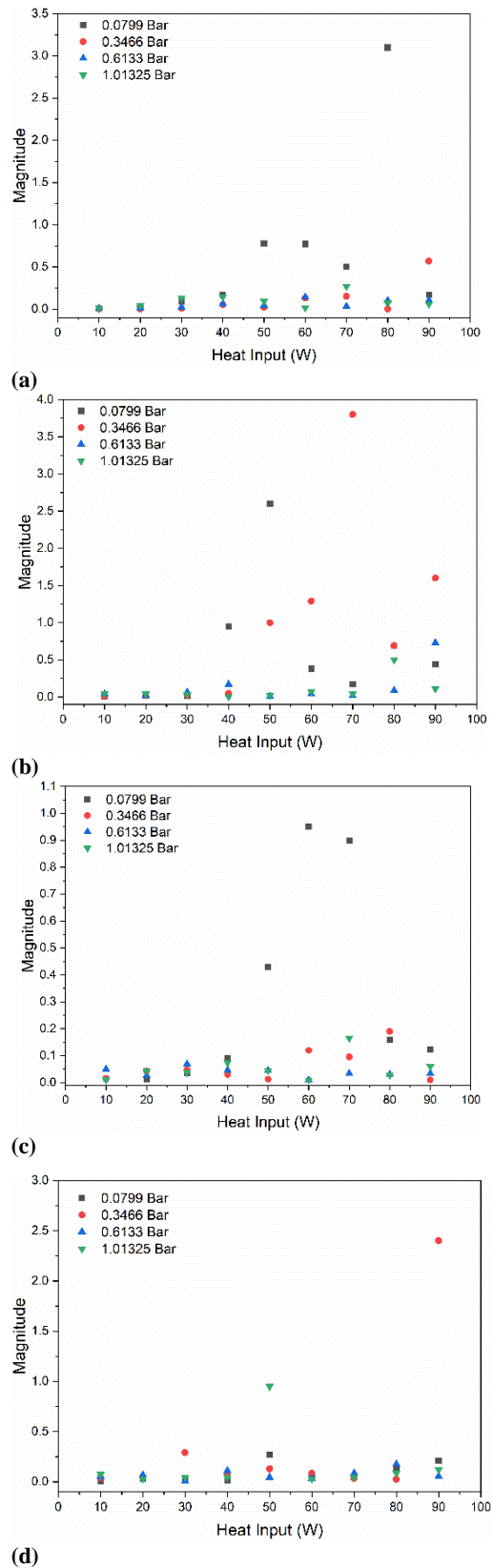


**Fig. 8. Dominant pulsation frequency magnitude variation for different evacuation pressure inside the condenser (a) at 30% FR (b) at 50% FR (c) at 70% FR (d) at 90%FR.**

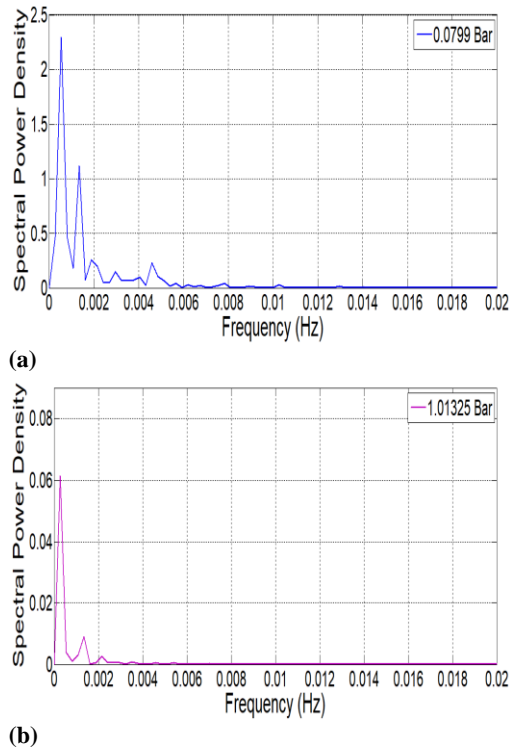


**Fig. 9. Power spectral density variation with frequency at (a) 0.0799 bar (b) 1.01325 bar evacuation pressure and 50% FR and 80W heat input.**

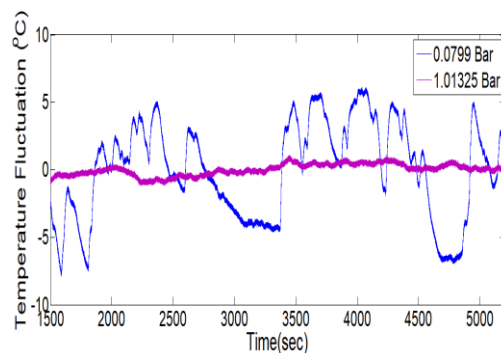


**Fig. 10. Temperature fluctuation with time for evacuation pressure at 50% FR and 80W heat input.**

- The higher heat resistance is found at lower heat input of 10W-20W because, at too low heat input the nanoparticles settle down in the evaporator section
- The time duration of the steady-state of the pulsating heat pipe is larger at low heat input of 10W and lesser at high heat input of 90W. The strong pulsating effect is observed at 50% FR.
- PHP's thermal resistance declines with rising heat input at the same evacuation pressure for different FR. The lowermost value of thermal resistance is perceived at 0.0799 bar evacuation pressure which is 0.132243 K/W, 0.116598K/W,

0.131791K/W and 0.125142K/W for 30%, 50%, 70% and 90% respectively.

- The effective thermal conductivity rises with rising heat input and evacuation pressure. The operating performance of the pulsating heat pipe is found better at 0.0799 bar evacuation pressure with the highest effective thermal conductivity value of 5078.337W/mK at 50% FR.
- The high pulsation frequency and temperature fluctuation are responsible for the better performance of pulsating heat pipe.

## REFERENCES

- Agha, S. R. (2011). Heat pipe performance optimisation: a Taguchi approach. *Collectors* 1, 4.
- Ahmad, H. H. and H. R. Rajab (2010). An Experimental Study of Parameters Affecting a Heat Pipe Performance. *Al-Rafidain Engineering Journal (AREJ)* 18(3), 97-117.
- Akachi, H. (1990). *U.S. Patent No. 4,921,041*. Washington, DC: U.S. Patent and Trademark Office.
- Akbari, A. and M. H. Saidi (2019). Experimental investigation of nanofluid stability on thermal performance and flow regimes in pulsating heat pipe. *Journal of Thermal Analysis and Calorimetry* 135(3), 1835-1847.
- Bao, K., X. Wang, Y. Fang, X. Ji, X. Han and G. Chen (2020). Effects of the surfactant solution on the performance of the pulsating heat pipe. *Applied Thermal Engineering* 178, 115678.
- Bastakoti, D., H. Zhang, D. Li, W. Cai and F. Li (2018a). An overview on the developing trend of pulsating heat pipe and its performance. *Applied Thermal Engineering* 141, 305-332.
- Bastakoti, D., H. Zhang, W. Cai and F. Li (2018b). An experimental investigation of thermal performance of pulsating heat pipe with alcohols and surfactant solutions. *International Journal of Heat and Mass Transfer* 117, 1032-1040.
- Çiloğlu, D. (2017). Thermal Behavior of Aqueous Cerium Oxide Nano-Suspension under the Pool Boiling Conditions, *Journal of the Institute of Science and Technology* 7(4), 181-8.
- Gupta, N. K., A. Barua, S. Mishra, S. K. Singh, A. K. Tiwari and S. K. Ghosh (2019). Numerical study of CeO<sub>2</sub>/H<sub>2</sub>O nanofluid application on thermal performance of heat pipe. *Materials Today: Proceedings* 18, 1006-1016.
- Harun, M. A., P. Gunnasegaran and N. A. Sidik (2019). Experimental study of loop heat pipe performance with nanofluids. *Journal of Advanced Research Design* 52 1(92), 13-27.

- Ji, Y., H. Ma, F. Su and G. Wang (2011a). Particle size effect on heat transfer performance in an oscillating heat pipe. *Experimental Thermal and Fluid Science* 35(4), 724-727.
- Ji, Y., C. Wilson, H. H. Chen and H. Ma (2011b). Particle shape effect on heat transfer performance in an oscillating heat pipe. *Nanoscale Research Letters* 6(1), 1-7.
- Jia, H., L. Jia and Z. Tan (2013). An experimental investigation on heat transfer performance of nanofluid pulsating heat pipe. *Journal of Thermal Science* 22(5), 484-490.
- Jung, C., J. Lim and S. J. Kim (2020). Fabrication and evaluation of a high-performance flexible pulsating heat pipe hermetically sealed with metal. *International Journal of Heat and Mass Transfer* 149, 119180.
- Kamel, M. S., O. Al-Oran and F. Lezsovits (2021). Thermal conductivity of Al<sub>2</sub>O<sub>3</sub> and CeO<sub>2</sub> nanoparticles and their hybrid-based water nanofluids: An experimental study. *Periodica Polytechnica Chemical Engineering* 65(1), 50-60.
- Khandekar, S. (2004). Thermo-hydrodynamics of closed loop pulsating heat pipes. Ph.D. thesis, University of Stuttgart, Germany.
- Kline, S. J. and F. A. McClintock (1953). Describing uncertainties in single-sample experiments. *Mechanical Engineering* 75, 3-8.
- Krishna, J., P. S. Kishore and A. B. Solomon (2017, August). Experimental study of thermal energy storage characteristics using heat pipe with nano-enhanced phase change materials. In *IOP Conference Series: Materials Science and Engineering* (Vol. 225, No. 1, p. 012058). IOP Publishing.
- Kwon, G. H. and S. J. Kim (2015). Experimental investigation on the thermal performance of a micro pulsating heat pipe with a dual-diameter channel. *International Journal of Heat and Mass Transfer* 89, 817-828.
- Li, Z., M. M. Sarafraz, A. Mazinani, H. Moria, I. Tlili, T. A. Alkanhal, M. Goodarzi and M. R. Safaei (2020). Operation analysis, response and performance evaluation of a pulsating heat pipe for low temperature heat recovery. *Energy Conversion and Management* 222, 113230.
- Liu, Y., H. Deng, J. Pfothner and Z. Gan (2015). Design of a hydrogen pulsating heat pipe. *Physics Procedia* 67, 551-556.
- Ma, H. B., C. Wilson, B. Borgmeyer, K. Park, Q. Yu, S. U. S. Choi and M. Tirumala, (2006). Effect of nanofluid on the heat transport capability in an oscillating heat pipe. *Applied Physics Letters* 88(14), 143116.
- Ma, H. B., C. Wilson, Q. Yu, K. Park, U. S. Choi and M. Tirumala (2006). An experimental investigation of heat transport capability in a nanofluid oscillating heat pipe. *ASME, Journal of Heat Transfer* 128(11), 1213-1216.
- Mameli, M., M. Marengo and S. Khandekar (2014). Local heat transfer measurement and thermo-fluid characterisation of a pulsating heat pipe. *International journal of thermal sciences* 75, 140-152.
- Nine, M. J., M. R. Tanshen, B. Munkhbayar, H. Chung and H. Jeong (2014). Analysis of pressure fluctuations to evaluate thermal performance of oscillating heat pipe. *Energy* 70, 135-142.
- Nazari, M. A., R. Ghasempour, M. H. Ahmadi, G. Heydarian and M. B. Shafii (2018). Experimental investigation of graphene oxide nanofluid on heat transfer enhancement of pulsating heat pipe. *International Communications in Heat and Mass Transfer* 91, 90-94.
- Naik, R., V. Varadarajan, G. Pundarika and K. R. Narasimha (2013). Experimental investigation and performance evaluation of a closed-loop pulsating heat pipe. *Journal of Applied Fluid Mechanics* 6(2), 267-275.
- Narasimha, K. R., S. N. Sridhara, M. Rajagopal, S. and K. N. Seetharamu (2012). Influence of heat input, working fluid, and evacuation level on the performance of pulsating heat pipe. *Journal of Applied Fluid Mechanics* 5(2), 33-42.
- Qu, J., F. Guan, Y. Lv and Y. Wang (2021). Experimental study on the heat transport capability of micro-grooved oscillating heat pipe. *Case Studies in Thermal Engineering* 26, 101210.
- Riehl, R. R. and N. dos Santos (2012). Water-copper nanofluid application in an open loop pulsating heat pipe. *Applied Thermal Engineering* 42, 6-10.
- Ramesh, R., P. Arulmozhi and M. Sathiskumar (2017). Experimental Analysis of Flat Plate Solar Water Heater using Cerium Oxide/Water Nano Fluid Under Forced Convection. *International Journal of Engineering Research & Technology* 6(6), 361-5.
- Shojaei, T. R., E. Khalife, M. Tabatabaei, B. Najafi and M. Mirsalim (2019). Effect of Nano-Cerium Oxide and Water Additives On B5 Combustion Emissions. *Zanco Journal of Pure and Applied Sciences* 31(s3), 34-39.
- Sun, C. H., C. Y. Tseng, K. S. Yang, S. K. Wu and C. C. Wang (2017). Investigation of the evacuation pressure on the performance of pulsating heat pipe. *International Communications in Heat and Mass Transfer* 85, 23-28.
- Taha-Tijerina, J. J. (2018). Thermal transport and challenges on nanofluids performance. *Microfluidics and Nanofluidics* 1, 215-256.
- Yadav, N. P., Madhuri and A. Kumar (2019),

- December). Parametric Behaviour of Closed Loop Pulsating Heat Pipe in the Presence of Water as a Working Fluid. In *Gas Turbine India Conference* (Vol. 83525, p. V001T03A017). American Society of Mechanical Engineers.
- Zufar, M., P. Gunnasegaran, K. C. Ng and H. B. Mehta (2019). Evaluation of the thermal performance of hybrid nanofluids in pulsating heat pipe. *CFD Letters* 11(11), 13-24.
- Zufar, M., P. Gunnasegaran, H. M. Kumar and K. C. Ng (2020). Numerical and experimental investigations of hybrid nanofluids on pulsating heat pipe performance. *International Journal of Heat and Mass Transfer* 146, 118887.